minerals

MDPI

Article

Arsenopyrite Dissolution and Bioscorodite Precipitation by *Acidithiobacillus ferrivorans* ACH under Mesophilic Condition

Sergio Barahona [1,2,†], Erick Herrera [1,3,†], Andrea Jara [1,2], Juan Castro-Severyn [1,4], Karem Gallardo [4], Gerardo Fuentes [5], Cristina Dorador [6], Claudia Saavedra [7] and Francisco Remonsellez [1,4,*]

1 Laboratorio de Microbiología del Desierto y Ambientes Extremos, Departamento de Ingeniería Química, Universidad Católica del Norte, Antofagasta 1240000, Chile; barahona.sergio.l@gmail.com (S.B.); eherrera.icm@gmail.com (E.H.); ajarasandoval@gmail.com (A.J.); jsevereyn@gmail.com (J.C.-S.)
2 Programa de Doctorado en Ingeniería de Procesos de Minerales, Facultad de Ingeniería, Universidad de Antofagasta, Antofagasta 1270300, Chile
3 Programa de Magister en Ciencias de la Ingeniería Mención Metalurgia, Universidad Católica del Norte, Antofagasta 1240000, Chile
4 Centro de Investigación Tecnológica del Agua en el Desierto-CEITSAZA, Universidad Católica del Norte, Antofagasta 1240000, Chile; kgallardo@ucn.cl
5 Universidad Tecnológica de Chile, INACAP, Santiago 8320000, Chile; gfuentesc@inacap.cl
6 Laboratorio de Complejidad Microbiana y Ecología Funcional, Departamento de Biotecnología, Facultad de Ciencias del Mar y Recursos Biológicos, Universidad de Antofagasta, Antofagasta 1270300, Chile; cristina.dorador@uantof.cl
7 Laboratorio de Microbiología Molecular, Facultad de Ciencias de la Vida, Universidad Andrés Bello, Santiago 8370186, Chile; csaavedra@unab.cl
* Correspondence: fremonse@ucn.cl
† These authors contributed equally to this work.

check for updates

Citation: Barahona, S.; Herrera, E.; Jara, A.; Castro-Severyn, J.; Gallardo, K.; Fuentes, G.; Dorador, C.; Saavedra, C.; Remonsellez, F. Arsenopyrite Dissolution and Bioscorodite Precipitation by *Acidithiobacillus ferrivorans* ACH under Mesophilic Condition. *Minerals* **2022**, *12*, 520. https://doi.org/10.3390/min12050520

Academic Editor: Naoko Okibe

Received: 28 January 2022
Accepted: 14 April 2022
Published: 22 April 2022

Abstract: Arsenopyrite is the most abundant arsenic-bearing sulfide mineral in the lithosphere, usually associated with sulfide gold ores. The recovery of this highly valuable metal is associated with the release of large quantities of soluble arsenic. One way to mitigate the effects of high concentrations of arsenic in solution is to immobilize it as scorodite precipitate, a more stable form. Hence, we addressed the scorodite formation capacity (under mesophilic conditions) of psychrotolerant *Acidithiobacillus ferrivorans* ACH isolated from the Chilean Altiplano. Bio-oxidation assays were performed with 1% arsenopyrite concentrate as unique energy source and produced solids were evaluated by X-ray diffraction (XRD) and QEMSCAN analysis. Interestingly, the results evidenced scorodite generation as the main sub-product after incubation for 15 days, due to the presence of the microorganism. Moreover, the QEMSCAN analysis support the XRD, detecting a 3.5% increase in scorodite generation by ACH strain and a 18.7% decrease in arsenopyrite matrix, implying an active oxidation. Finally, we presented the first record of arsenopyrite oxidation capacity and the stable scorodite production ability by a member of *A. ferrivorans* species under mesophilic conditions.

Keywords: arsenopyrite; *Acidithiobacillus ferrivorans*; bioscorodite; precipitation; bio-oxidation

1. Introduction

Arsenopyrite (FeAsS) is the most abundant arsenic-bearing sulfide mineral in the lithosphere, whereby it has become important for the mineral processing industries that have been focusing their interest on finding new technologies to recover commercially valuable metals such as copper, nickel, and gold from these ores with lower economic and energy costs [1,2]. Low grade refractory sulfide gold ores are usually associated with high amounts of pyrite and arsenopyrite. In such ores, gold is dispersed as submicroscopic particles and the efficient recovery of this finely dispersed metal is very difficult by conventional methods (e.g., cyanidation) without pretreatment [3]. In this context, the bio-oxidation of refractory sulfide gold ores prior to cyanidation could be one alternative

pretreatment. The bio-oxidation enhances gold particles liberation from the sulfide matrix, increasing the metal recovery [4,5]. Bio-oxidation pretreatment of refractory sulfide ores prior to cyanidation represents a successful application of biohydrometallurgy, which has been successfully practiced in several mining industries in Africa, Australia, South America and Asia [4]. However, the bio-oxidation of arsenopyrite concentrates in turn increases the soluble arsenic levels, which could strongly affect the microbial activity and the bio-oxidation processes could be completely arrested [6].

The scorodite ($FeAsO_4 \cdot 2H_2O$) is a crystalline ferric arsenate with low solubility in aqueous solutions, relatively high stability and excellent dewatering characteristics; therefore, it is considered the ideal way to discard arsenic in mining industries [7]. Conventionally, the scorodite can be either produced by a chemical process such as hydrothermal precipitation or by controlled precipitation under atmospheric pressure [7,8]. Both precipitation processes require high As(V) [9–11]; however, as the leaching progresses, the soluble As(III) concentration increases, exceeding the As(V), making the scorodite precipitation gradually more inefficient in batch process [12].

As the As(III) concentrations are predominant in these As-bearing compounds/solutions, novel technologies for metallurgical operations are required for their treatment. Hence, a promising alternative is the microbial scorodite crystallization. Moreover, the bioscorodite ($FeAsO_4$ $2H_2O$) generation was demonstrated using the iron oxidizing archaea *Acidianus sulfidivorans* in presence of 1.9 g/L of arsenate at 80 °C. Furthermore, the produced bioscorodite showed similar physico-chemical characteristics to those obtained from chemical process, without the need of As(III) oxidation pretreatments [13]. On the other hand, a mixed culture of Archaea belonging to the *Sulfolobales* order was used to produce bioscorodite in an airlift reactor (at 72 °C) yielding 3 g/g of arsenic removal [14]. Additionally, Okibe and collaborators described that the archaea *Acidianus brierleyi* was capable of oxidizing arsenite (As(III)) to arsenate (As(V)), producing bioscorodite (at 70 °C) without the presence of any chemical oxidant [15]. Indeed, this microorganism was capable of oxidizing ferrous iron (Fe(II)) and arsenite (As(III)) simultaneously to ferric iron (Fe(III)) and arsenate (As(V)) using atmospheric oxygen as electron acceptor, under thermophilic conditions [16].

Given the precipitation process requires high temperatures, most of the reported investigations has been carried out using thermoacidophilics microorganisms. Nevertheless, the biomineralization of scorodite during oxidative processing of arsenic-rich cobalt minerals at mesophilic temperatures has been demonstrated using microbial consortia including iron and sulfur-oxidizing mesophilic and thermotolerant prokaryotes [17]. Hence, the capacity of scorodite synthesis by mesophilic organisms like *Acidithiobacillus* is poorly understood. This genus is composed by seven species (*A. albertensis, A. caldus, A. thiooxidans, A. ferrooxidans, A. ferrivorans, A. ferriphilum* and *A. ferridurans*) which differ from each other by their tolerance ranges to pH, temperature, heavy metals, and energy source used. Specifically, *Acidithiobacillus ferrivorans* is a unique psychrophilic member of this genus (capable of growth at 4–30 °C) and uses iron sulfur or reduced inorganic sulfur compounds as energy source [18]. Additionally, several groups have described the presence of this microorganism in diverse cold environments from Russia, Norway, USA, China, Peru and Chile [18–23]. Nevertheless, the focus of these previous reports has been the psychrotolerance features, but with little focus on understanding the arsenic resistance and scorodite synthesis capacities. Therefore, in this work, we aimed to evaluate the arsenopyrite refractory mineral dissolution capacity by *Acidithiobacillus ferrivorans* ACH under mesophilic conditions, and to determine the arsenic removal ability from As-bearing minerals to precipitate it as bioscorodite.

2. Materials and Methods

2.1. Bacterial Strain and Growth Conditions

A. ferrivorans ACH was isolated from an enrichment culture obtained from a shallow acid stream (pH < 3) located at 4000 m.a.s.l in the Chilean Altiplano (Cerro Aroma River-Tarapacá Region) [20]. This strain is capable of growing in the presence of iron,

sulfur and pyrite as energy source and exhibited a broad range of growth temperatures ranging between 4–28 °C [24], and it is also able to tolerate high Cu(II) concentrations [25]. Following this, *A ferrivorans* ACH was cultured at 28 °C with 120 rpm of constant agitation in modified 1X Mackintosh (MAC) medium (50X, per liter): 50 mM $(NH_4)_2SO_4$; 26.65 mL H_2SO_4; 7.8 mM K_2HPO_4; 6.2 mM $MgCl_2 \cdot 6H_2O$; 50 mM $CaCl_2 \cdot 2H_2O$ and 50 mL of trace elements [26].

2.2. Bio-Oxidation Experiments

The bio-oxidation experiments were performed in 500 mL Erlenmeyer shake flasks containing 200 mL of MAC medium with 1% arsenopyrite pulp (concentrate) as energy source and 10% bacterial inoculum; incubated for 20 days at 28 °C with 120 rpm of constant agitation. The arsenopyrite concentrate was obtained from the "Comercializadora de Minerales Viacha" mining company (La Paz–Bolivia, Ciudad de la Paz, Bolivia). Next, bacterial growth was monitored by planktonic unstained cell counting by phase-contrast microscope (CX21, Olympus, Tokyo, Japan) using a Neubauer chamber. Additionally, the redox potential and pH values were measured by an Ag/AgCl electrode (Model 420A, ORION, Shanghai, China). As and Fe total in solution during the bio-oxidation assays were obtained using Perkin Elmer Optima 7000 DV model inductively coupled plasma optical emission spectrometry (ICP-OES, Waltham, MA, USA). The assays were set to recollect the produced solids after 5, 10, 15 and 20 days of incubation. Additionally, control assays were prepared exactly the same without the bacteria. Three independent experiments with at less three technical replicates each were performed.

2.3. Mineralogical Characterization

The control of arsenopyrite pulp and the bio-oxidation solid products were characterized by mineralogical identification through different approaches: (i) X-ray diffraction was carried out with a diffractometer (D5000, Siemens, Munich, Germany). The powder patterns were analyzed using DiffracPlus and TOPAS (Total Pattern Analysis Software). Crystalline phases were identified using the database of the International Center for Diffraction Data (ICDD); (ii) X-ray fluorescence using a spectrometer (SRS 3000, Siemens); (iii) Quantitative Evaluation of Minerals by Scanning Electron Microscopy analysis—QEMSCAN® (E430, CSIRO, Canberra, Australia) and (iv) Dual optical microscopy (BX51, Olympus, Japan).

2.4. Search for Arsenic Resistance Genetic Determinants in the ACH Strain Genome

Some known and described arsenic response genes for the *Acidithiobacillus* genus were used as reference and queried to identify their presence in the ACH strain genome (GeneBank Accesion: GCA_018854855.1) using BLAST.

3. Results

3.1. Characterization of Arsenopyrite Concentrate

The preliminary analysis of the arsenopyrite showed a chemical composition of 27.7% iron, 32.1% arsenic and 18.8% sulfur. In parallel, through optical microscopy, we visualized the mineralogical species present at the sample (Figure 1), which was composed mainly by arsenopyrite and pyrite (Figure 1A,B,D), while chalcopyrite and gold particles were detected in a minor proportion (Figure 1B,C).

Sample	% Fe	% As	% S
Arsenopyrite	27.7	32.1	18.8

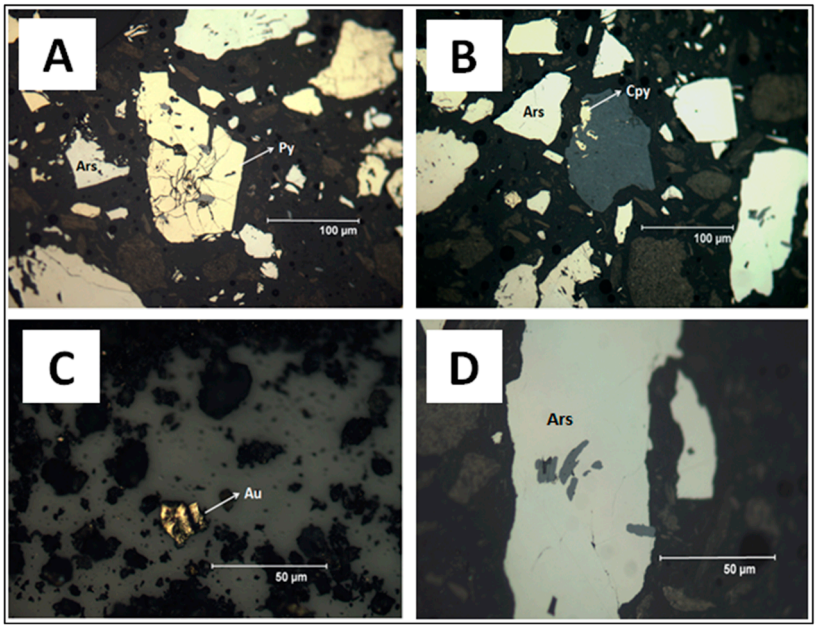

Figure 1. Chemical characterization of arsenopyrite through atomic absorption spectrophotometry (upper table) and visualization in an optical microscopy (lower image panels: (**A**–**D**)). The white arrows indicate the detected mineral species. Ars: arsenopyrite; Py: pyrite; Au: gold; Cpy: chalcopyrite.

Additionally, to corroborate the aforementioned results, we performed an X-ray diffraction (XRD) to the same arsenopyrite pulp to estimate mineralogical composition. The diffractogram pattern evidenced the presence of arsenopyrite, pyrite and quartz as the main mineralogical species in the sample. The major proportion detected was for arsenopyrite with 38.9% followed by pyrite (24.4%) and quartz with a minor proportion of 5.5% (Figure 2).

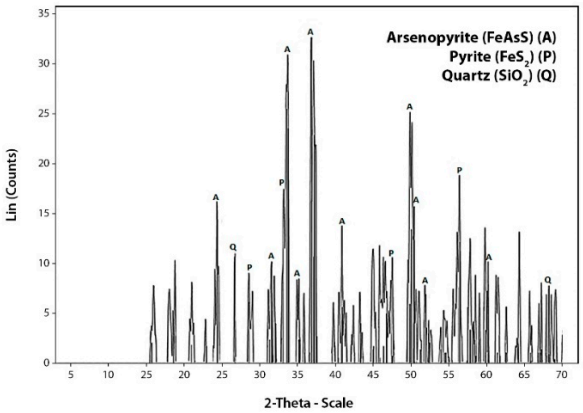

Figure 2. Diffractogram of arsenopyrite pulp used for the experimental bio-oxidation assays. Obtained through X-ray diffractometry analyzed with TOPAS Software.

In addition, through X-ray fluorescence spectrophotometry we estimated that the sample contained trace amounts of nickel (Ni), cobalt (Co), antimony (Sb), copper (Cu), zinc (Zn), lead (Pb) and bismuth (Bi) (Table 1).

Table 1. Trace elements of arsenopyrite pulp estimated by X-ray fluorescence spectrophotometry.

Trace Elements	Ni	Co	Sb	Cu	Zn	Pb	Bi
Amounts (ppm)	16.71	7.08	671.00	165.00	605.00	138.00	582.00

3.2. Growth of A. ferrivorans ACH Cells Using Arsenopyrite as Energy Source

First, the ACH strain cells were initially adapted to grow in the presence of different pulp concentrations of arsenopyrite (1, 5, 10 and 12%, respectively; Figure 3) and the growth rate was negatively affected by concentrations higher than 5%. Additionally, the iron oxidation capacity decreased, evidenced by the low redox potential values in 5, 10 and 12% pulp concentrations (361 mV, 318 mV and 300 mV, respectively; Figure 3). On the other hand, the pH values remained close to 1.8 in presence of 1% pulp, while at higher concentrations of pulp, pH values remained close to 1.8 (Figure 3). Hence, the best growth rate was obtained with the 1% pulp condition (Figure 4). Furthermore, the cell growth (exponential phase) started after 5 days of lag phase, reaching between 5.0×10^6–3.2×10^7 cell mL^{-1}, increasing one order of magnitude after 20 days incubation of growth. Besides, the redox potential value also increased up to 560 mV by this time (Figure 4). Thus, according to these results, a 1% pulp was selected as experimental condition for the bio-oxidation assays.

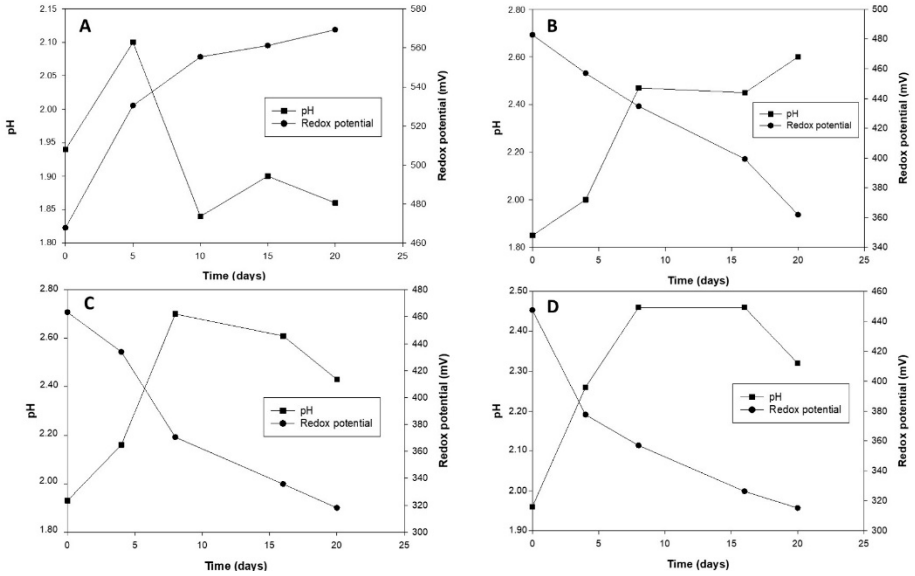

Figure 3. Bio-oxidation of arsenopyrite by *A. ferrivorans* ACH cells in presence of 1% (**A**), 5% (**B**), 10% (**C**) and 12% (**D**) arsenopyrite pulp at mesophilic condition.

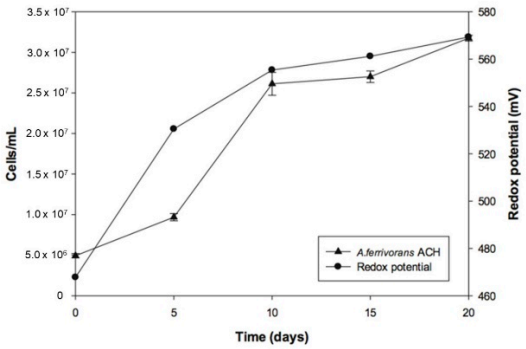

Figure 4. Bio-oxidation of arsenopyrite by *A. ferrivorans* ACH cells. The cells were grown in presence of 1% arsenopyrite pulp at mesophilic condition. The cells number and the redox potential were monitored every 5 days. Mean values (n = 3) are plotted.

3.3. Arsenopyrite Dissolution and Bioscorodite Precipitation by A. ferrivorans ACH

Solid residues recovered from *A. ferrivorans* ACH bio-oxidation experiments were characterized by optical microscopy, XRD and QEMSCAN. The dissolution of arsenopyrite concentrates by ACH action was evidenced by optical microscopy from day 15 onwards, as we saw the unperturbed mineral structure for the first 10 days (Figure 5A,B). However, after 15 days, the arsenopyrite structure drastically changed, displaying an irregular surface, due to microbial activity (Figure 5C). Finally, after 20 incubation days, arsenopyrite looked almost completely dissolved (Figure 5D). This could potentially enhance the release of more valuable components contained in this refractory matrix.

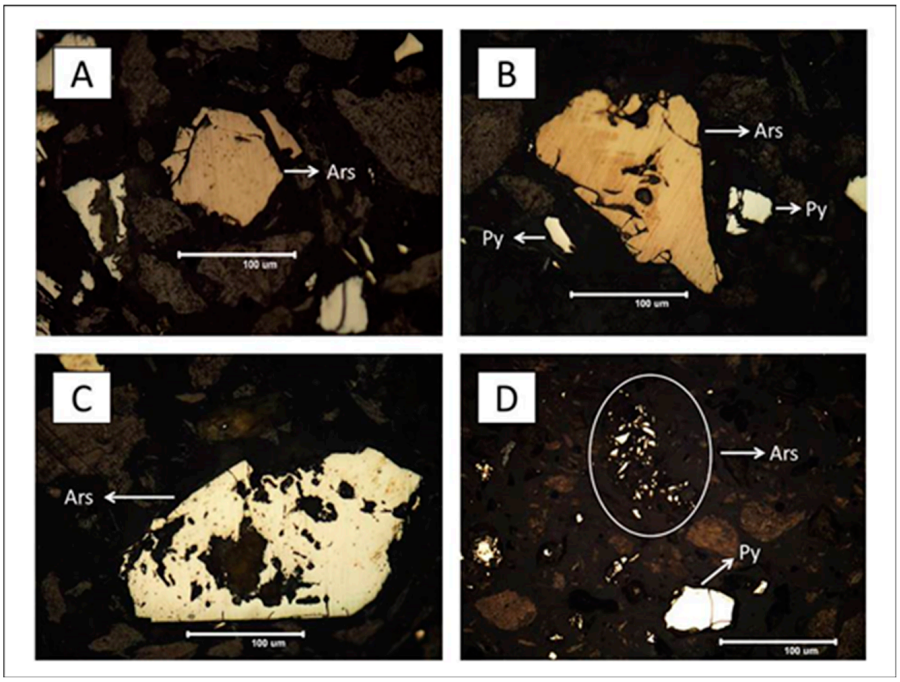

Figure 5. Arsenopyrite dissolution by *A. ferrivorans* ACH cells during 20 days of incubation. Optical microscopy images at: (**A**) 5 days; (**B**) 10 days; (**C**) 15 days and (**D**) 20 days. The white arrows show the mineral species detected (Ars: arsenopyrite and Py: pyrite).

Similarly, the XRD pattern suggests that after 5 days of incubation arsenopyrite was the predominant solid, without any significant change in the mineral matrix (Figure 6A), despite the fact that an increase in the redox potential values was detected at this period of time (Figure 4). Subsequently, after 10 days of incubation, the XRD pattern showed changes in the pulp mineral species, detecting arsenopyrite, elemental sulfur and pyrite (Figure 6B). Interestingly, after 15 days of incubation, the XRD patterns revealed the presence of bioscorodite ($FeAsO_4$ $2H_2O$), in addition to arsenopyrite, pyrite, elemental sulfur and quartz (Figure 6C). Therefore, the bioscorodite precipitated is produced due to the bacterium ability to oxidize both iron and arsenic contained in the arsenopyrite, generating a stable precipitate which is rich in both elements. Finally, after 20 incubation days, the XRD result show that scorodite is one predominant mineral species in the culture, produced under mesophilic conditions (Figure 6D).

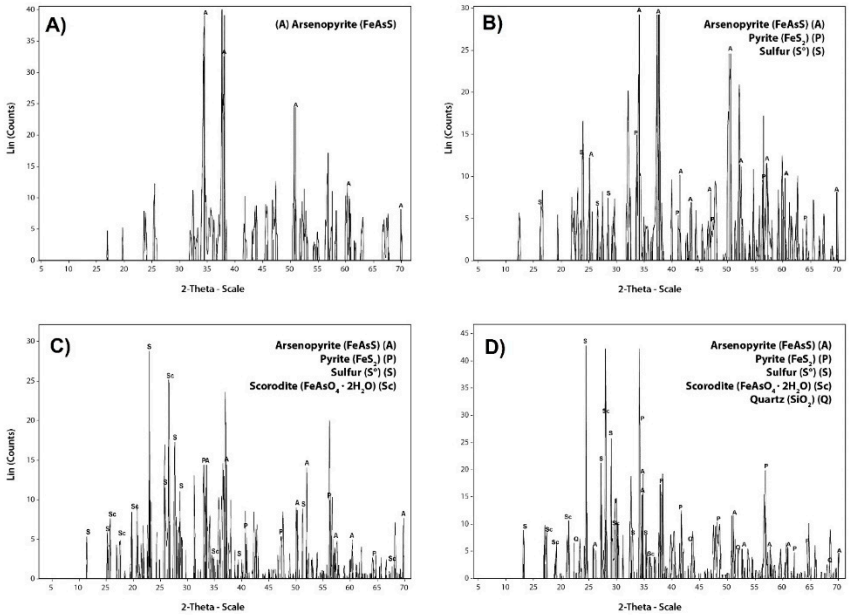

Figure 6. XRD patterns for arsenopyrite dissolution assays with *A. ferrivorans* ACH at 1% density of pulp. (**A**): 5 days of incubation; (**B**): 10 days of incubation; (**C**): 15 days of incubation; (**D**): 20 days of incubation.

Additionally, we performed a QEMSCAN analysis on both the arsenopyrite pulp and the solids obtained during bio-oxidation assays to estimate the percent of arsenopyrite dissolution and bioscorodite generation by the ACH strain activity. Firstly, the results for the pulp composition supports those of X-ray fluorescence indicating arsenopyrite as the main sulfide mineral in the sample with 35.5% followed by other As-Fe-Ni sulfides (15.1%) and nickel/cobalt associated arsenopyrite sulfides (13.5%) (Table 2). Secondly, the ACH strain was capable of dissolving the arsenopyrite matrix from 35.5% to 16.8% after 20 days of incubation. In addition, the microorganism was capable of dissolving other types of arsenopyrite such as those associated with nickel and cobalt (13.5% to 1.1%), and other arsenic sulfides (Table 2).

Table 2. Mineralogical composition of the arsenopyrite pulp and the solids obtained after bio-oxidation of arsenopyrite by *A. ferrivorans* ACH using a QEMSCAN analysis.

Mineral Mass (%)	Arsenopyrite Pulp without Bacteria	Bio-Oxidation Process			
		5 Days	10 Days	15 Days	20 Days
Alloys As-Fe	2.2	0.7	0.5	0.9	0.8
Arsenopyrite	35.5	37.7	31.0	23.0	16.8 *
Arsenopyrite (Ni+Co)	13.5	12.8	9.2	4.2	1.1 *
As-Ni-Fe Sulfides	3.6	2.4	2.8	0.8	1.0 *
As-Fe-Ni Sulfides	15.1	12.3	8.0	2.2	0.3 *
As-bearing Pyrite	1.0	1.5	1.8	2.3	2.9
As-bearing sulfates	7.4	11.4	17.4	32.0	32.1 +
As-bearing silicates	4.1	3.9	5.8	7.0	9.8 +
Scorodite	1.9	2.5	3.3	4.7	5.4 +
Others As minerals	0.1	0.2	0.5	0.9	2.1 +
Pyrite	10.6	9.4	12.1	13.8	15.8
Others	5.0	5.0	8.0	8.0	12.0

*: minerals species with decreased mass percent. +: minerals species with increased mass percent.

It is important to highlight the mineral mass appearance of As-bearing sulfates, reaching 32% after 15 days of incubation. Interestingly, the scorodite synthesis by the presence of ACH strain was also determined, increasing the mineral mass from 1.9% to 5.4% (Table 2), which corroborates the patterns obtained previously by XRD.

Finally, we determined the As and Fe concentrations in solution after the arsenopyrite bio-oxidation assays (Figure 7). We observed an increase in total Fe and As concentration over time, both concomitant with the grow of *A. ferrivorans* ACH showed previously (Figure 4). This potential means that the ACH strain is capable of tolerating higher concentrations of arsenic; however, the respective tolerance tests, as determined by Minimal Inhibitory Concentrations (MIC), are pending a future study.

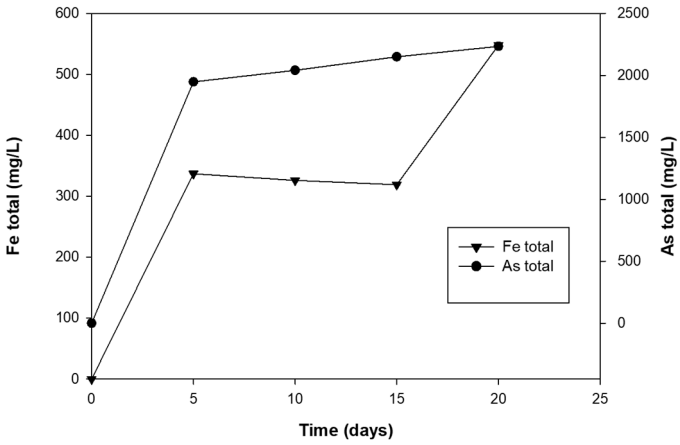

Figure 7. Determination of As and Fe total in solution during the bio-oxidation assays to 1% arsenopyrite by *A. ferrivorans* ACH.

4. Discussion

Some authors have described that the rates of oxidation and dissolution for sulfide minerals (such as arsenopyrite) are enhanced by microorganism metabolic processes, because they could use those to generate energy [27–29]. The ability of those organisms has led to their use for mineral ores pretreatment, which include sulfide ores containing valuable metals such as gold [29]. Thus, the arsenopyrite dissolution by microorganisms has been previously reported by many authors [27,28,30]. Additionally, four mechanisms of action for arsenopyrite dissolution have been suggested according to the following equations:

$$2FeAsS + 2.5O_2 + 2H_2SO_4 + H_2O \rightarrow 2FeSO_4 + 2H_3AsO_3 + 2S^0 \quad (1)$$

$$2FeSO_4 + 0.5O_2 + H_2SO_4 \rightarrow Fe_2(SO_4)_3 + H_2O \quad (2)$$

$$2FeAsS + 5Fe_2(SO_4)_3 + 6H_2O \rightarrow 12FeSO_4 + 2H_3AsO_3 + 3H_2SO_4 + 2S^0 \quad (3)$$

$$2S^0 + 2H_2O + 3O_2 \rightarrow 2H_2SO_4 \quad (4)$$

The microorganism grows initially on the surface of arsenopyrite where ferrous iron (as $FeSO_4$), arsenite (as arsenous acid (H_3AsO_3)) and elemental sulfur are generated (Equation (1)). Later, due to increased concentrations of ferrous iron (Fe^{+2}), the microorganisms are capable of oxidizing this to ferric iron (Fe^{+3}) (Equation (2)). Then, the ferric iron (as $Fe_2(SO_4)_3$) generated by the microorganism is used for attaching (chemically) to the mineral surface producing ferrous iron, arsenite, sulfuric acid and elemental sulfur (Equation (3)). Finally, the elemental sulfur (S^0) turns into sulfuric acid to maintain the low pH values required by the microorganisms (Equation (4)) [31].

The principal microorganisms involved in arsenopyrite dissolution are acidophilic, iron and/or sulfur oxidizing and capable of resisting high arsenic concentration in solution [29]. In this context, here we reported for the first time the capacity of *Acidithiobacillus*

ferrivorans to use arsenopyrite concentrate as energy source under mesophilic conditions. However, previous studies have described this species as a psychrotolerant, able to oxidize iron, sulfur, and reduced inorganic sulfur compounds, and to solubilize pyrite as energy source [18,19,24]. Moreover, the capacity to grow using arsenopyrite as unique energy source by ACH strain is evidenced in Figure 4, where the increase in bacterial cellular density is one order of magnitude after 20 days of incubation. In addition, the increased redox potential was concomitant with the proliferation of cell number detected in our assays (Figure 4). Therefore, it can be suggested that bacteria promote an active oxidation of the arsenopyrite concentrate reported previously in some group of archaea such as *Sulfobacillus* and *Acidianus.* In the particular case of the *Acidithiobacillus* genus, previous reports determined the capacities of arsenic resistance, specifically in some *A. ferrooxidans* strain grown in the presence of arsenopyrite [32,33], suggesting that this genus is tolerant to arsenic. In addition, mixed mesophilic adapted culture (enriched in *A. caldus* and *L. ferriphilum*) have shown high tolerance to arsenic in packed-bed columns and continuous bioleaching reactors of arsenopyrite from mine tailings [34,35].

Bacterial attachment on minerals increases leaching activities due to a higher interaction space between the cells and mineral surface [36], enhancing the oxidation of refractory minerals such as arsenopyrite. In this context, our results show the real capacity of ACH strain to oxidize arsenopyrite, dissolving almost entirely the matrix by action of the ferric iron generated by the microorganisms after 15 days (Equation (2)) (Figure 5). In addition, microorganism's presence generates more drastic changes on the arsenopyrite surface compared to the use of a $Fe_2(SO_4)_3$ chemical solution [37]. On the other hand, depending on the oxidizing conditions, a great number of sub-products could be generated from the arsenopyrite oxidation, which could inhibit the correct mineral oxidation due to the formation of surface passivation layers [30]. Additionally, these passivation layers might be composed by elemental sulfur, arsenolite, jarosite, iron hydroxides, amorphous ferric arsenate/scorodite and ferric phosphate [38]. Therefore, to describe these sub-products and understand their possible negative effects, a combination of different approaches (X-ray diffraction (XRD), scanning electron microscopy (SEM) and QEMSCAN) was the most convenient strategy to analyze the surface chemistry during arsenopyrite bio-oxidation.

Interestingly, the XRD patterns revealed that the principal sub-products generated by ACH strain were sulfur, pyrite and scorodite (Figure 6). Additionally, a similar result reported the presence of ferric arsenates and sulfur on bio-oxidized arsenopyrite by *Acidthiobacillus ferrooxidans* [27]. Additionally, the transformation of arsenopyrite to jarosite, sulfur and ferric arsenate when metabolized by *Acidithiobacillus caldus* at 45 °C was described [38]. Nevertheless, in none of these cases was scorodite identified; only an unidentified, amorphous ferric arsenate was reported. Likewise, the formation of jarosite, sulfur and silica were reported due the presence of *A. thiooxidans*, due to a mine tailing (mainly composed by arsenopyrite) oxidation [39]. Additionally, similar results using two different moderate thermophile bacterial consortia (1: *Sulfobacillus thermosulfidooxidans* with *A. caldus*, and 2: *Ferroplasma thermophilum* with *A. caldus*) were described, for which jarosite and sulfur were the main sub-products generated in both cases [31].

Additionally, the comparative oxidation of arsenopyrite employing three different systems evidenced the sulfur formation in all the cases. Nevertheless, only in the acidic systems (sterile acid) was scorodite formation detected after 18 days of incubation [40]. In our work, jarosite formation was not detected; one possible reason is the assays parameters, such as pH values (below 3 but above 1.5) (Figure 3), as the formation of this compound requires lower pH values (pH 1.5) [41]. In addition, the QEMSCAN analysis performed to the solids generated by *A. ferrivorans* ACH arsenopyrite oxidation corroborate the previously XRD obtained results, detecting a 5.4% scorodite formation after 20 days and an 18.7% arsenopyrite matrix decrease (Table 2). Additionally, we identified an increase in As-bearing sulfate generated by *A. ferrivorans* ACH, detecting 32.1% after 20 days. These results could be attributed to the formation of some precipitate of sulfates such as tooelite ($Fe_6(AsO_3)_4(SO_4)(OH)_4{\cdot}4H_2O$), a ferric arsenic sulfate generated by some

microorganisms capable of oxidizing ferrous iron and not arsenite [42], like our strain. The biogenic of tooelite by several *A. ferrooxidans* strains (CC1, B5, B20 and the type strain ATCC 23270) which depend on iron rate oxidation was reported; however, the biogenic tooelite mechanisms have not been elucidated to date [43].

The microorganism ability to oxidize arsenopyrite should imply their capacity to tolerate high concentrations of soluble arsenic. In our case, we propose that the ACH strain can tolerate concentrations over 2 g/L of As, because we determined the As and Fe concentrations in solution after the arsenopyrite bio-oxidation assays (Figure 7). We observed that the increase in total Fe over time is concomitant with bacterial growth (Figure 4), and as the oxidation process takes place, the bacteria could tolerate higher arsenic concentrations (Figure 7). It is important to mention that this is the first report describing the ability of an *A. ferrivorans* species member to grow in arsenopyrite concentrate, in turn generating scorodite under mesophilic conditions. Moreover, a preliminary analysis of the *A. ferrivorans* ACH genome revealed the presence of the *ars* operon involved in arsenic resistance, in the five genes conformation: *arsA*, arsenical pump-driving ATPase; *arsD*, arsenical resistant operon trans-actin repressor; *arsC*, arsenate reductase; *arsR*, arsenical resistant operon repressor; *arsB*, arsenic efflux pump (Supplementary Table S1) [44]. Hence, the presence of this classical arsenic resistance operon would provide to the ACH strain the necessary functional potential to cope with toxic environmental arsenic concentrations. Moreover, the main mechanism relies on the arsenate (As(V)) reduction to arsenite (As(III)) by ArsC, for its later expulsion by ArsB. Nevertheless, the presence of an arsenite oxidase was not detected, like in others *Acidithiobacillus* genus strain [32], which would be responsible for the As(III) to As(V) oxidation, which is required for the ferric arsenate (scorodite) precipitate formation at low pH values [12,15]. However, we have to consider thermodynamic aspects: at low pH values, the arsenite (As(III)) is found as arsenous acid (H_3AsO_3), which should be easily oxidized to arsenate (As(V)) (as arsenic acid, H_3AsO_4) by the ferric ions action, according to the following equation:

$$H_3AsO_3 + Fe^{3+} + H_2O \rightarrow H_3AsO_4 + Fe^{2+} + 2H^+ \quad (5)$$

Nevertheless, some authors have reported that the kinetics of the reaction is very slow and almost no oxidation of As(III) occurs [45]. Conversely, other authors described that in presence of pyrite, the reaction speed increase and the oxidation of As(III) to As(V) can be observed [46]. Thus, this observation aligns with our results due to presence of pyrite (Figure 6 and Table 2). In other words, the capacity of the ACH strain to oxidize pyrite, could favor the As(III) to As(V) oxidation (Equation (5)) as it has been reported before [23]. Additionally, the higher concentration of biogenic ferric iron would allow scorodite precipitation (Equation (6)) [45].

$$Fe_2(SO_4)_3 + 2H_3AsO_4 + 2H_2O \rightarrow 2FeAsO_4 \cdot 2H_2O_{(scorodite)} + 3H_2SO_4 \quad (6)$$

The role of microorganisms is mainly to keep high the redox potential (Eh > 450 mV) and a high concentration of ferric ion in the solution, catalyzing the reoxidation of ferrous ion [45]. The chemical mechanisms described previously could be answer as to why the ACH strain is capable of generating scorodite (biogenic) despite not having an arsenite oxidase in his genome, potentially enhancing its use in bio-oxidation processes of refractory ore.

5. Conclusions

In this study, we provided the first evidence of arsenopyrite concentrate oxidation capacity conducted by the psychrotolerant iron-sulfur oxidizing *A. ferrivorans* ACH under mesophilic condition reducing from 35.5% to 16.8% arsenopyrite matrix. This strain was effectively adapted to high concentrations of As, which was reflected in As concentrations quantified after the bio-oxidations assays, in turn generating scorodite as sub-products of the reaction, this being the most stable ways to discard arsenic in mining industries.

Our ACH strain was capable of generating 5.4% bioscorodite after 20 days of incubation. On the other hand, we demonstrated that higher pulp concentration effects their bio-oxidation capabilities, with 1% being the best pulp concentrations assayed. In general, the bio-oxidation of the gold-containing sulfide ores is used as a pretreatment which can decrease the consumption of lixiviants used for gold solubilization in subsequent parts of the operation, ultimately increasing the gold yields. The results of this study suggest the feasibility of using *A. ferrivorans* ACH to remove As from As-rich minerals under mesophilic condition, as an alternative to conventional processes actually employed at higher temperature. Future studies in this area are required to understand the resistance mechanisms used by microorganisms to thrive under adverse conditions, which could be coupled with other advantageous capacities (as bioscorodite precipitation), generating biotechnological applications to solve industrial problems with a focus on the efficient use of natural resources, and minimizing environmental impacts.

Supplementary Materials: The following supporting information can be downloaded at: https://www.mdpi.com/article/10.3390/min12050520/s1, Table S1: Sequence of arsenic proteins identified in *A. ferrivorans* ACH genome.

Author Contributions: S.B., E.H., G.F. and F.R. conceived and designed the study. S.B., E.H. and A.J. performed the microbiological experiments. S.B., E.H. and A.J. processed the samples and performed the chemistry experiments. F.R., G.F. and C.D. contributed reagents and materials. S.B., J.C.-S., A.J., F.R., C.D., C.S. and K.G. wrote the manuscript. All authors have read and agreed to the published version of the manuscript.

Funding: This work was supported by ANID (Agencia Nacional de Investigación y Desarrollo de Chile). SB was funded by ANID Doctoral Scholarship (ANID PCHA/Doctorado Nacional 2015-21150614) and project CORFO ING2030 16EN12-71940 (Assistant Investigator). AJ was funded by ANID Doctoral Scholarship (ANID PCHA/Doctorado Nacional 2017-21171060). JCS was funded by PostDoctoral FONDECYT 3210156. KG was funded by project CORFO ING2030 16EN12-71940. CS was funded by ANID-FONDECYT Regular 1210633 and ECOS-ANID 170023. FR was funded by PMI 1795 project (Programa de Mejoramiento Institucional en Recursos Hídricos 1795).

Institutional Review Board Statement: Not applicable.

Informed Consent Statement: Not applicable.

Data Availability Statement: Not applicable.

Acknowledgments: The authors acknowledge Scientific Equipment Unit-MAINI of the Universidad Católica del Norte.

Conflicts of Interest: The authors declared no conflict of interest.

References

1. Brierley, C.L. Biohydrometallurgical prospects. *Hydrometallurgy* **2010**, *104*, 324–328. [CrossRef]
2. Panda, S.; Akcil, A.; Pradhan, N.; Deveci, H. Current scenario of chalcopyrite bioleaching: A review on the recent advances to its heap-leach technology. *Bioresour. Technol.* **2015**, *196*, 694–706. [CrossRef] [PubMed]
3. Cassity, W.; Pesic, B. Interactions of *Thiobacillus ferrooxidans* with arsenite, arsenate and arsenopyrite. In *Proceedings of Biohydrometallurgy and the Environment toward the Mining of the 21st Century, Part I*; Amils, R., Ballester, A., Eds.; Elsevier: Amsterdam, The Netherlands, 1999; pp. 521–532.
4. Ndlovu, S. Biohydrometallurgy for sustainable development in the African minerals industry. *Hydrometallurgy* **2008**, *91*, 20–27. [CrossRef]
5. Fashola, M.; Ngole-Jeme, V.; Babalola, O. Review Heavy metal pollution from gold mines: Environmental effects and bacterial strategies for resistance. *Int. J. Environ. Res. Public Health* **2016**, *13*, 1047. [CrossRef]
6. Tuffin, I.; de Groot, P.; Deane, S.; Rawlings, D. An unusual Tn21-like transposon containing an ars operon is present in highly arsenic resistant strains of the biomining bacterium *Acidithiobacillus caldus*. *Microbiology* **2005**, *151*, 3027–3039. [CrossRef]
7. Shibata, E.; Onodera, N.; Fujita, T.; Nakamura, T. Elusion tests of scorodite synthesized by oxidation of ferrous ions. *Resour. Process.* **2012**, *59*, 42–48. [CrossRef]
8. Caetano, M.L.; Ciminelli, V.S.T.; Rocha, S.D.F.; Spitale, M.C.; Caldeira, C.L. Batch and continuous precipitation of scorodite from dilute industrial solutions. *Hydrometallurgy* **2009**, *95*, 44–52. [CrossRef]

9. Paktunc, D.; Dutrizac, J.; Gertsman, V. Synthesis and phase transformations involving scorodite, ferric arsenate and arsenical ferrihydrite: Implications for arsenic mobility. *Geochim. Cosmochim. Acta* **2008**, *72*, 2649–2672. [CrossRef]
10. Dutrizac, J.; Jambor, J. The synthesis of crystalline scorodite, FeAsO2x 2H2O. *Hydrometallurgy* **1988**, *19*, 377–384. [CrossRef]
11. Monhemius, A.; Swash, P. Removing and stabilizing as from copper refining circuits by hydrothermal processing. *JOM* **1999**, *51*, 30–33. [CrossRef]
12. Tanaka, M.; Okibe, N. Factors to Enable Crystallization of Environmentally Stable Bioscorodite from Dilute As(III) Contaminated Waters. *Minerals* **2018**, *8*, 23. [CrossRef]
13. Gonzalez-Contreras, P.; Weijma, J.; van der Weijden, R.; Buisman, C.J.N. Biogenic scorodite crystallization by *Acidianus sulfidivorans* for arsenic removal. *Environ. Sci. Technol.* **2010**, *44*, 675–680. [CrossRef]
14. Gonzalez-Contreras, P.; Weijma, J.; Buisman, C.J.N. Bioscorodite crystallization in an airlift reactor for arsenic removal. *Cryst. Growth Des.* **2012**, *12*, 2699–2706. [CrossRef]
15. Okibe, N.; Koga, M.; Morishita, S.; Tanaka, M.; Heguri, S.; Asano, S.; Sasaki, K.; Hirajima, T. Microbial formation of crystalline scorodite for treatment of As(III)-bearing copper refinery process solution using Acidianus brierleyi. *Hydrometallurgy* **2014**, *143*, 34–41. [CrossRef]
16. Higashidani, N.; Kaneta, T.; Takeyasu, N.; Shoji Motomizu, S.; Okibe, N.; Sasaki, K. Speciation of arsenic in a thermos acidophilic iron-oxidizing archaeon, Acidianus brierleyi, and its culture medium by inductively coupled plasma–optical emission spectroscopy combined with flow injection pretreatment using an anion-exchange mini-column. *Talanta* **2014**, *122*, 240–245. [CrossRef]
17. Johnson, D.B.; Dybowska, A.; Schofield, P.F.; Herrington, R.J.; Smith, S.L.; Santos, A.L. Bioleaching of arsenic-rich cobalt mineral resources, and evidence for concurrent biomineralisation of scorodite during oxidative bio-processing of skutterudite. *Hydrometallurgy* **2020**, *195*, 105395. [CrossRef]
18. Hallberg, K.; González-Toril, E.; Johnson, D. *Acidithiobacillus ferrivorans*, sp. nov.; facultatively anaerobic, psychrotolerant iron-, and sulfur-oxidizing acidophiles isolated from metal mine-impacted environments. *Extremophiles* **2010**, *14*, 9–19. [CrossRef]
19. Kimura, S.; Bryan, C.; Hallberg, K.; Johnson, D. Biodiversity and geochemistry of an extremely acidic, low-temperature subterranean environment sustained by chemolithotrophy. *Environ. Microbiol.* **2011**, *13*, 2092–2104. [CrossRef]
20. Barahona, S.; Dorador, C.; Remonsellez, F. Identification and characterization of a psychrotolerant Acidithiobacillus strain from Chilean Altiplano. *Adv. Mater. Res.* **2013**, *825*, 74–78. [CrossRef]
21. Talla, E.; Hedrich, S.; Mangenot, S.; Ji, B.; Johnson, D.; Barbe, V.; Bonnefoy, V. Insights into the pathways of iron- and sulfur-oxidation, and biofilm formation from the chemolithotrophic acidophile *Acidithiobacillus ferrivorans* CF27. *Res. Microbiol.* **2014**, *165*, 753–760. [CrossRef]
22. Ccorahua-Santos, R.; Eca, A.; Abanto, M.; Guerra, G.; Ramírez, P. Physiological and comparative genomic analysis of *Acidithiobacillus ferrivorans* PQ33 provides psychrotolerant fitness evidence for oxidation at low temperature. *Res. Microbiol.* **2017**, *168*, 482–492. [CrossRef]
23. Peng, T.; Ma, L.; Feng, X.; Tao, J.; Nan, M.; Liu, Y.; Li, J.; Shen, L.; Wu, X.; Yu, R.; et al. Genomic and transcriptomic analyses reveal adaptation mechanisms of an *Acidithiobacillus ferrivorans* strain YL15 to alpine acid mine drainage. *PLoS ONE* **2017**, *12*, e0178008. [CrossRef]
24. Barahona, S.; Dorador, C.; Riuyong, Z.; Aguilar, P.; Sand, W.; Vera, M.; Remonsellez, F. Isolation and characterization of a novel *Acidithiobacillus ferrivorans* strain from the Chilean Altiplano: Attachment and biofilm formation on pyrite at low temperature. *Res. Microbiol.* **2014**, *165*, 782–793. [CrossRef]
25. Barahona, S.; Castro-Severyn, J.; Dorador, C.; Saavedra, C.; Remonsellez, F. Determinants of copper resistance in *Acidithiobacillus ferrivorans* ACH isolated from the Chilean Altiplano. *Genes* **2020**, *11*, 844. [CrossRef]
26. Mackintosh, M. Nitrogen fixation by *Thiobacillus ferrooxidans*. *J. Gen. Microbiol.* **1978**, *105*, 215–218. [CrossRef]
27. Fernandez, M.; Mustin, C.; de Donato, P.; Barres, O.; Marion, P.; Berthelin, J. Occurrences at mineral-bacterial interface during oxidation of arsenopyrite by *Thiobacillus ferrooxidans*. *Biotechnol. Bioeng.* **1995**, *46*, 13–21. [CrossRef]
28. Corkhill, C.; Vaughan, D. Arsenopyrite oxidation—A review. *Appl. Geochem.* **2009**, *24*, 2342–2361. [CrossRef]
29. Kaksonen, A.; Mudunuru, B.; Hackl, R. The role of microorganisms in gold processing and recovery—A review. *Hydrometallurgy* **2014**, *142*, 70–83. [CrossRef]
30. Dave, S.; Gupta, K.; Tipre, D. Characterization of arsenic resistant and arsenopyrite oxidizing *Acidithiobacillus ferrooxidans* from Hutti gold leachate and effluents. *Bioresour. Technol.* **2008**, *99*, 7514–7520. [CrossRef]
31. Deng, S.; Gu, G.; Wu, Z.; Xu, X. Bioleaching of arsenopyrite by mixed cultures of iron-oxidizing and sulfur-oxidizing microorganisms. *Chemosphere* **2017**, *185*, 403–411. [CrossRef] [PubMed]
32. Butcher, B.; Deane, S.; Rawling, D. The chromosomal arsenic resistance genes of *Thiobacillus ferrooxidans* have an unusual arrangement and confer increased arsenic and antimony resistance to Escherichia coli. *Appl. Environ. Microbiol.* **2000**, *66*, 1826–1833. [CrossRef] [PubMed]
33. Duqesne, K.; Lebrun, C.; Casiot, O.; Bruneel, J.; Personne, C.; Leblanc, M.; Elbaz-Poulichet, F.; Morin, G.; Bonnefoy, V. Immobilization of arsenite and ferric iron by *Acidithiobacillus ferrooxidans* and its relevance to acid mine drainage. *Appl. Environ. Microbiol.* **2003**, *69*, 6165–6173. [CrossRef] [PubMed]
34. Ngoma, E.; Borja, D.; Smart, M.; Shaik, K.; Kim, H.; Petersen, J.; Harrison, S.T.L. Bioleaching of arsenopyrite from Janggun mine tailings (South Korea) using an adapted mixed mesophilic culture. *Hydrometallurgy* **2018**, *181*, 21–28. [CrossRef]

35. Borja, D.; Nguyen, K.M.; Silva, R.A.; Ngoma, E.; Petersen, J.; Harrison, S.T.L.; Park, J.H.; Kim, H. Continuous bioleaching of arsenopyrite from mine tailings using an adapted mesophilic microbial culture. *Hydrometallurgy* **2019**, *187*, 187–194. [CrossRef]
36. Rohwerder, T.; Sand, W. Oxidation of inorganic sulfur compounds in acidophilic prokaryotes. *Eng. Life. Sci.* **2007**, *7*, 301–309. [CrossRef]
37. Fomchenko, N.V.; Muravyov, M.I. Thermodynamic and XRD analysis of arsenopyrite biooxidation and enhancement of oxidation efficiency of gold-bearing concentrates. *Int. J. Miner. Process.* **2014**, *133*, 112–118. [CrossRef]
38. Tuovinen, O.; Bhatti, T.; Bigham, J.; Garcia, O.; Lindstrom, E. Oxidative dissolution of arsenopyrite by mesophilic and moderately thermophilic acidophiles. *Appl. Environ. Microbiol.* **1994**, *60*, 3268–3274. [CrossRef]
39. Lee, E.; Han, Y.; Park, J.; Hong, J.; Rene ASilva, R.; Kim, S.; Kim, H. Bioleaching of arsenic from highly contaminated mine tailings using *Acidithiobacillus thiooxidans*. *J. Environ. Manag.* **2015**, *147*, 124–131. [CrossRef]
40. Deng, S.; Gu, G.; Xu, B.; Li, L.; Wu, B. Surface characterization of arsenopyrite during chemical and biological oxidation. *Sci. Total Environ.* **2018**, *626*, 349–356. [CrossRef]
41. Meruane, G.; Vargas, T. Bacterial oxidation of ferrous iron by *Acidithiobacillus ferrooxidans* in the pH range 2.5–7.0. *Hydrometallurgy* **2003**, *71*, 149–158. [CrossRef]
42. Wang, X.; Qingzhu, L.; Qi, L.; Yuchen, Y.; Xia, J.; Qiuhong, L.; Qingwei, W.; Yanjie, L. Arsenic(III) biotransformation to tooeleite associated with the oxidation of Fe(II) via *Acidithiobacillus ferrooxidans*. *Chemosphere* **2020**, *248*, 126080. [CrossRef]
43. Egal, M.; Casiot, C.; Morin, G.; Parmentier, M.; Bruneel, O.; Lebrun, S.; Elbaz-Poulichet, F. Kinetic control on the formation of tooeleite, schwertmannite and jarosite by *Acidithiobacillus ferrooxidans* strains in an As(III)-rich acid mine water. *Chem. Geol.* **2009**, *265*, 432–441. [CrossRef]
44. Slyemi, D.; Bonnefoy, V. How prokaryotes deal with arsenic. *Env. Microbiol. Rep.* **2012**, *4*, 571–586. [CrossRef]
45. Wiertz, J.; Magda, M.; Escobar, B. Mechanism of pyrite catalysis of As(III) oxidation in bioleaching solutions at 30 °C and 70 °C. *Hydrometallurgy* **2006**, *83*, 35–39. [CrossRef]
46. Tao, J.; Qian, L.; Yong-bin, Y. Bio-oxidation of arsenopyrite. *Trans. Nonferrous Met. Soc. China* **2008**, *18*, 1433–1438.